Signed online chromatic-dispersion monitoring by synchronous detection of FM-induced arrival-time modulations in the clock-recovery phase-locked loop

Reinhold Noé, David Sandel, Suhas Bhandare, Frank Wüst, Biljana Milivojevic, and Vitali Mirvoda

University of Paderborn, EIM-E, Optical Communication and High-Frequency Engineering, Warburger Strasse 100, D-33098 Paderborn, Germany

noe@upb.de

RECEIVED 28 OCTOBER 2003; REVISED 20 MAY 2004; ACCEPTED 7 JUNE 2004; PUBLISHED 00 JULY 2004

Chromatic dispersion (CD) in optical single-mode fibers, i.e., the wavelength dependence of the propagation delay, distorts pulses and is a big problem in 10- and 40-Gbit/s transmission systems. Adjustable drop-in CD compensators require an online CD detection. For this purpose, we modulate the optical power of the laser in a 40-Gbit/s transmitter by 1.2% (rms) at a frequency of 5 MHz. In the presence of CD, the associated periodic optical frequency variation modulates the signal arrival time, which is measured by synchronous (lock-in) detection of an error signal in the clock recovery of the receiver. CD as large as -268 to $+350$ ps/nm is detected including its sign, more than by any comparable technique. The uncertainty of measured arrival-time modulations can be as low as 100 attoseconds. Moreover, no extra optics or high-frequency electronics are needed, which makes this method extremely cheap to implement. Results are given for nonreturn to zero and CSRZ, intensity modulation, and differential phase-shift keying.

OCIS codes: 060.4510, 060.2270.

1. Introduction

Chromatic dispersion (CD) of existing optical single-mode fiber links is a big obstacle for the deployment of 10- and 40-Gbit/s transmission equipment.[A] Even in dispersion-compensated long-haul fiber links, the temperature and wavelength dependence of CD may be problematic. Network operators would therefore like to have adjustable, drop-in CD compensators. For automatic operation of these, online CD detection is required, including its sign. Most reported CD detection schemes (e.g., Refs. [1–6]) need extra optical filters, fibers, receivers, and/or high-frequency electronics. Given the strict cost awareness of the telecommunication industry, these are unlikely to be affordable.

A similar problem, the detection of polarization-mode dispersion, has recently been solved in a simple manner [7]: The signal parameter that influences the propagation delay, i.e., the state of polarization, was modulated at a low speed. In the receiver, the clock-recovery signals were analyzed to detect the associated arrival-time modulation. Here we apply this principle to CD, for intensity modulation and for differential phase-shift keying (DPSK) [8, 9].

A In Abstract, pls. define CS

2. Principle

The complex field transfer function of an optical fiber with a length L is $\underline{H}(\omega) = e^{-j\beta(\omega)L}$, where ω is the optical angular frequency and attenuation has been neglected. It is useful to approximate its phase by a truncated Taylor series, $\varphi = -\beta(\omega)L = -\left[\beta + (\omega-\omega_0)\beta' + (1/2)(\omega-\omega_0)^2\beta''\right]L$. At ω_0, the propagation constant $\beta(\omega)$ assumes the value β, and its first and second derivatives with respect to ω are β' and β'', respectively. The group delay $\tau_g = -\varphi' = [\beta' + (\omega-\omega_0)\beta'']L$ is a linear function of ω. Its derivative with respect to wavelength λ and length L is the CD coefficient

$$D = \frac{d^2\tau_g}{d\lambda dL} = -\frac{2\pi c}{\lambda^2}\beta'',$$

$\sim$17 ps/(nm·km) in SSMF.[B] The dimensionless index γ is defined as

$$\gamma = \frac{DL\lambda^2}{T^2\pi c},$$

(Ref. [10]), where T is the bit duration. To better understand the effects of CD, consider a small-signal sinusoidal amplitude modulation with a frequency $(\omega-\omega_0)/(2\pi) = 1/(2T)$ equal to the Nyquist frequency of a data signal. It is converted into pure phase modulation if there is a $\pi/2$ phase shift of the sidebands with respect to the carrier. This requires $(1/2)(\omega-\omega_0)^2\beta''L = \pm\pi/2$ or $|\gamma| = 2/\pi$. The values $|\gamma| = 0.252$ and $|\gamma| = 0.218$ cause 1-dB eye-closure penalties in intensity- and DPSK-modulated systems, respectively, for the nonreturn-to-zero (NRZ) signal format [10].

A small pump current modulation of a distributed-feedback (DFB) laser will modulate the optical power and also the optical frequency. At low frequencies, there can be a considerable phase lag between pump current and frequency modulation because the latter depends not only on the carrier density but likewise on the chip temperature, which is modulated by the pump current with an intrinsic delay. In the presence of CD, a frequency excursion δf causes an arrival time delay of

$$\delta\tau_g = -\delta f\frac{DL\lambda^2}{c} = -\delta f T^2\gamma\pi.$$

It can be neglected in comparison with the eye closure as long as $|\delta f T| \ll 1$, and hence $|\delta\tau_g/T| \ll |\gamma\pi|$, holds. In the following, this will be the case. It means that the small-signal modulation frequency may be chosen so high that it is outside the phase-locked loop (PLL) bandwidth of the clock recovery in the receiver.

3. Chromatic-Dispersion Detection in an Intensity-Modulated System

Figure 1 details a transmission setup. 40-Gbit/s data are 16 : 1 multiplexed from 2.5-Gbit/s, $2^{23}-1$ pseudorandom binary sequence (PRBS) data streams with mutual delays of 8 bits. The signal drives a $LiNbO_3$ intensity modulator to modulate the signal of a transmitter laser using the NRZ modulation format. Alternatively the CSRZ format is used. For this purpose, an additional $LiNbO_3$ intensity modulator between laser and data modulator is driven by a 20-GHz sinusoid, thereby generating $\sim$ 13-ps-long pulses with alternating polarities and 40-GHz repetition frequency. A small pump current modulation of the DFB transmitter laser at 5 MHz results in a 1.2% (rms) amplitude modulation and in an optical frequency modulation with a 224-MHz (rms) deviation. In the clock and data recovery (CDR, from

B What does SSMF stand for?

Infineon), a clock-phase detector takes the difference of two correlation products, one between the decision circuit output signal and the output signal of an auxiliary decision circuit that is clocked $T/2$ later, and a similar one between the decision-circuit output signal corresponding to the next bit (delay T) and the auxiliary signal. If the clock phase is optimally chosen, each correlation product will on average assume half of its maximum value because the auxiliary decision circuit is clocked exactly in between two subsequent bits. The clock-phase error signal is fed to a proportional-integral controller (PI). Its output signal controls the voltage-controlled oscillator (VCO, from WORK Microwave GmbH). Since a sinusoidal clock-phase error signal is expected, the controller output signal is likewise sinusoidal, just shifted in phase.

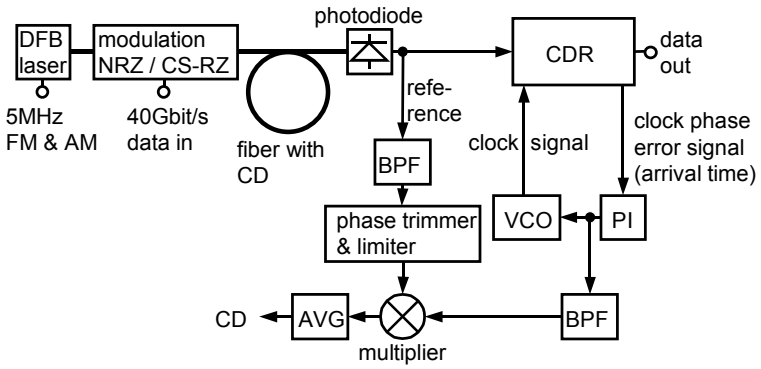

Fig. 1. Experimental setup for CD detection.

A timing reference is conveniently obtained by detecting the parasitic amplitude modulation. Parasitic amplitude modulation (AM) is contained in a low-frequency copy of the detected photocurrent. Just like the differentiated arrival time, it is bandpass filtered (BPF). After being amplitude limited, it serves as a reference, with a phase that is adjusted for best sensitivity. The arrival-time signal is synchronously detected with a multiplier and averaged (AVG). Amplitude and sign of the averaged signal represent the CD. Although Fig. 1 explains the principle, signals were in reality processed digitally, and an extra low-frequency photodiode was employed to detect the amplitude modulation (AM).

40-Gbit/s data were transmitted with no significant degradation introduced by the laser FM. Bit error rate (BER) measurement failed only when the eye pattern was closed owing to CD. Actual CD values of fibers under test were measured separately using a tunable laser and an oscilloscope triggered from the transmitter side. For NRZ, the usable measurement range was $DL = -268 + \cdots + 350\,\mathrm{ps/nm}$. SSMF was used for positive, DSF for negative dispersion. Erbium-doped fiber amplifiers (EDFAs) were added when needed. Figure 2 shows Fourier coefficients in the complex plane. Each point represents a measurement interval of $154\,\mu\mathrm{s}$, and each cloud of points stands for one CD value. The smaller $|DL|$ is, the smaller the standard deviation within a cloud. By synchronous demodulation (lock-in detection), all values are projected along the horizontal axis.

Figure 3 shows these CD readings as a function of the actual CD. Not only is the sign of CD correctly detected for all cases, but the readout is even monotonous. For larger CD, the clock-recovery PLL failed to lock. The measurement range corresponds to $\gamma = -1.09, \ldots, 1.43$ for NRZ. To our knowledge, this is the largest signed online CD measurement range reported to date. Similar results were obtained for CSRZ but the measurement range was restricted to $DL = -125, \ldots, 170\ \mathrm{ps/nm}$ ($\gamma = -0.51, \ldots, 0.69$). However, CSRZ is more susceptible to CD than NRZ owing to the shorter pulses. Figures 4 and 5 show re-

ceived eye diagrams in a monitor photodiode for both modulation formats at different CD values.

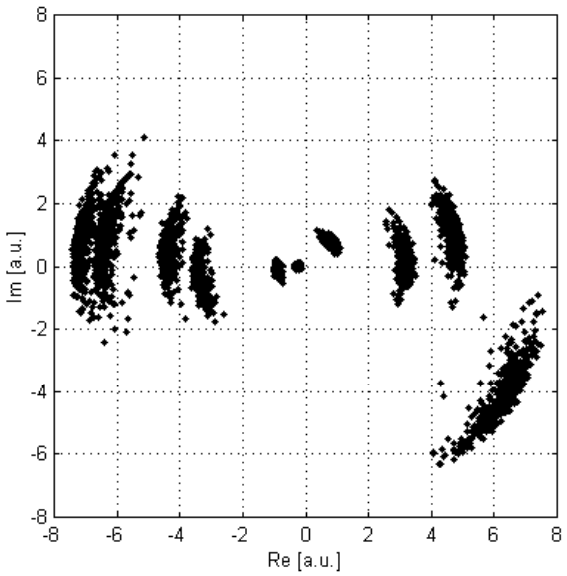

Fig. 2. 5-MHz Fourier coefficients of arrival time in the complex plane for various CD values.

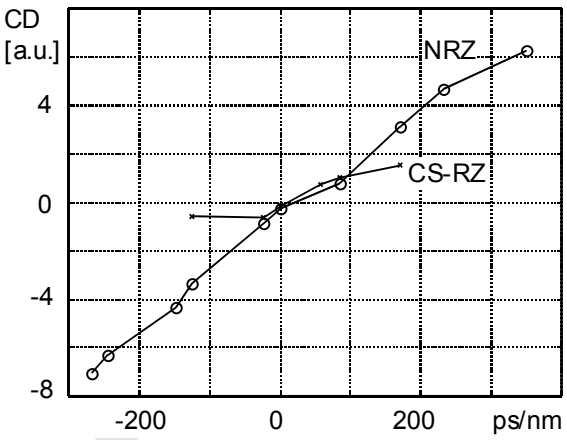

Fig. 3. Measured CD [a.u] versus actual CD.

Owing to the synchronous detection, the sign of CD is correctly obtained. CD compensation could therefore be readily accomplished if a compensator with adjustable DGD were connected to the measured CD signal via a simple integrator.

Next the detection noise for zero actual CD (no dispersive fiber) was investigated for various measurement interval durations. A number of samples was taken in each case. This allowed estimation of the measured CD standard deviation. Figure 6 shows these values, expressed as CD values using the scale factors defined by the curve slopes in Fig. 3. For

C Author: What does DGD stand for?

measurement intervals of 616 μs, the CD standard deviation is below 1 ps/nm. This value is considered to be tolerable. As a consequence, CD compensation with a time constant < 1 ms seems feasible. When measured over 314 ms, the measured CD standard deviation is ~ 50 fs/nm. The corresponding 5-MHz spectral component of the arrival-time modulation equals ~ 100 attoseconds (rms). This sensitivity is due to a good voltage-controlled oscillator (VCO) frequency stability and the synchronous detection of the arrival-time variations.

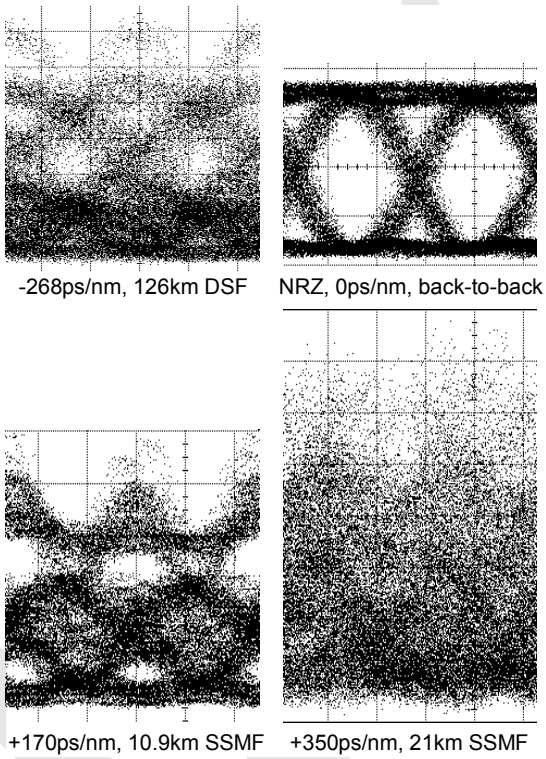

Fig. 4. Received eye diagrams for NRZ signal format.

In practice, long-term stability of the CD readout is a decisive quality criterion. In an experiment (with intensity modulation, but using another setup that was also later used for DPSK modulation), the drift was recorded with zero nominal CD over 9 h in unattended operation (Fig. 7, top trace left). The CD readout was stable within ± 600 fs/nm. Later the same experiment was run during 63 h over a weekend (Fig. 7, long trace). However, a significant room-temperature change occurred during that interval. The associated drift of the (uncontrolled) modulator bias point moved the crossover level of the eye diagram. This caused the CD readout to change by 18 ps/nm. At the end of the experiment, the modulator bias point was readjusted blindly, i.e., without looking at the CD readout, simply by adjusting the eye diagram to look the same as at the beginning of the experiment. After this readjustment, the CD readout was less than 1.5 ps away from the original CD readout. We believe that the achievable long- term stability with controlled modulator bias point is better than ± 5 ps/nm, even though our optical frequency deviation is quite low.

The CDR itself possesses two decision circuits clocked in antiphase at 20 GHz, and the 40-Gbit/s eye diagram exhibits a nonnegligible 2-bit periodicity owing to patterning in

the last 2:1 part of the electrical multiplexer. Depending on even or odd bits being directed to one particular output of the first $1:2$ electrical demultiplexer, the offset changes by several ps/nm (< 5 ps/nm). Although this is not much, one is not forced to live with this uncertainty. In order to measure the offset, we have added a cycle slipping circuit into the PLL. It contains a monoflop and can inject short pulses having a certain temporal integral into the control part of the PLL. When there is such a pulse, the PLL temporarily falls out of lock and relocks with one single cycle slip, 25 ps in our case. This allows identification of the different CD readout offsets. Once this is done, the PLL stays locked in a particular configuration. The offset between the mean of the CD readouts measured in both locked states and the CD readout measured in the chosen locked state can be taken into account. As a result, each corrected CD readout represents the mean CD readout of both locked states. A very similar feature (with averaging over 16 locked states) was already implemented for the measurements of Fig. 7.

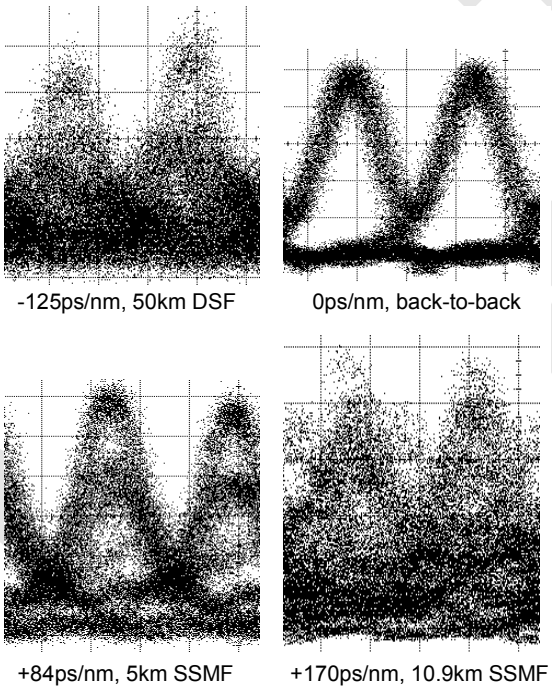

Fig. 5. Received eye diagrams for CSRZ signal format.

The polarity of the offset stays unchanged if there is fiber CD at the first locking. So, an offset-compensated CD measurement and compensation system would operate as follows:

1. Lock the PLL, and measure CD.
2. Induce one cycle slip, and measure CD again.
3. Determine whether the locking status (2) represents the even or the odd channel. Look into a table that tells the CD offset applicable at zero nominal CD for that channel.
4. Continue CD measurements, correct them by that offset, switch the CD control loop on, and wait until CD is fully compensated.

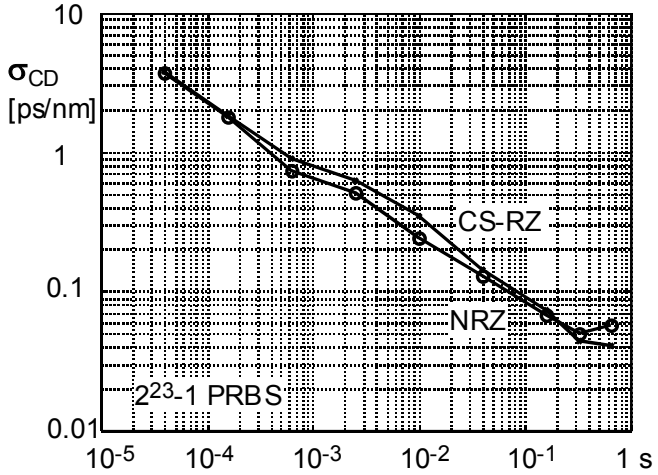

Fig. 6. Standard deviation of measured CD versus measurement interval, at zero actual dispersion.

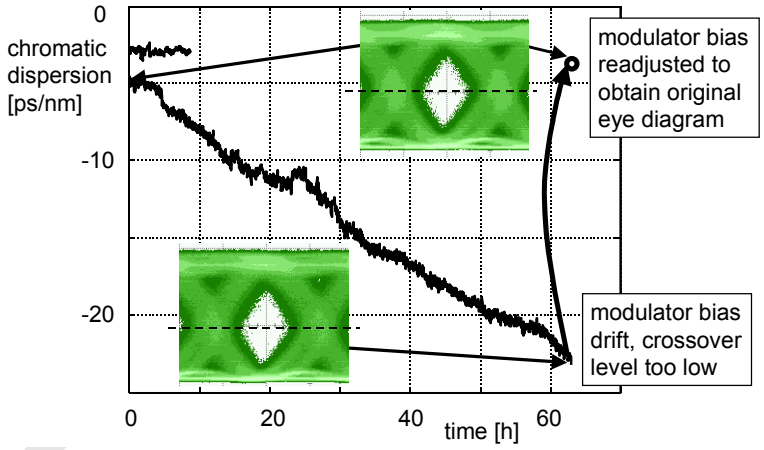

Fig. 7. Measured CD at zero actual CD versus time.

Only a cycle slip and one CD measurement are needed in addition to what is needed in any system of this kind. The extra time needed could be of the order of some milliseconds or so. The CD compensation system will have a larger time constant anyway, and therefore the extra delay does not matter . Note that the extra time delay occurs only once, when the transmitted signal is found for the first time by the receiver.

It is also to be kept in mind that the overall CD readout uncertainty of Fig. 7 is still less than ± 5 ps/nm, which is more than sufficient for practical applications.

The power dependence was also assessed. The CD readout changes by 11 ps/nm per 100% of optical power variation. For the measurement of Fig. 7, the optical power was therefore stabilized by an automatic EDFA pump current adjustment. Otherwise, the optical power could be measured in view of a feed-forward correction of the measured CD.

In an earlier stage of the experiments, the modulation frequency dependence of the measured CD standard deviation was investigated for the NRZ signal format (Fig. 8). An old experimental CDR was used that had a clock-phase detector, where only one correlation product was determined and subtracted from an offset. Sensitivities are therefore not directly comparable with Fig. 6. The measurement interval was 154μs. The large noise for low modulation frequencies is due to VCO phase noise. For a $2^7 - 1$ PRBS, the sensitivity keeps increasing as the modulation frequency increases. For the $2^{23} - 1$ PRBS, it levels off beyond 1.67 MHz, owing to patterning.

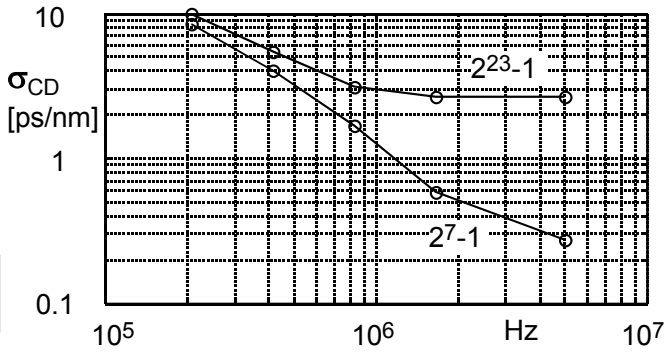

Fig. 8. Standard deviation of measured CD versus modulation frequency for NRZ, measured in 154 μs.

4. Chromatic-Dispersion Detection in a Differentially Phase-Shift Keyed System

CSRZ-DPSK is a high-performance optical transmission scheme [11]. CD monitoring will be required especially to cancel residual CD of trunk lines with positive and negative dispersion fibers. Arrival-time detection of CD as outlined above is a challenge here because optical DPSK receivers are frequency selective.

The 40-Gbit/s CSRZ-DPSK transmitter (Fig. 9) employs a 16 : 1 multiplexer (Infineon), amplifiers for the 20-GHz half-rate clock, a $LiNbO_3$ CSRZ pulse carver (Triquint), modulator drivers (SHF communications), and a $LiNbO_3$ data modulator (Triquint). The signal was transmitted through various fibers.

In the receiver, after passing an EDFA and an optical filter, the signal enters a commercial Mach–Zehnder interferometer wth a 100-s delay. This allows differential encoding at 10 Gbit/s in the transmitter [11]. In our system, differential encoding was not implemented nor needed because a $2^7 - 1$ PRBS was transmitted.

The interferometer outputs are connected to two photodiodes (u2t). The signal is demultiplexed in a 1:16 clock-and-data recovery (Infineon) with differential inputs. All

2.5-Gbit/s subchannels are bit error free, with almost identical sensitivities. The half-rate clock signals in transmitter and receiver are generated by dielectric resonator VCOs (WORK Microwave GmbH).

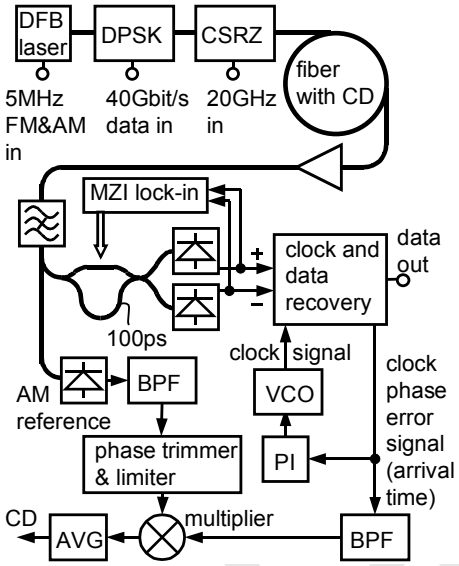

Fig. 9. 40-Gbit/s CSRZ-DPSK transmission setup.

Parts of the photodiode output signals are tapped off and sent through differential 40-Gbit/s amplifiers (Infineon) for subsequent ac power detection (not shown). Maximum rf power is observed when the interferometer phase difference is set correctly. The phase difference is therefore thermally modulated at 400 Hz and is stabilized by integrating the lock-in detected output signal of the rf power detector.

The 400-Hz lock-in stabilization of the interferometer phase essentially eliminates the effect of a small polarization dependence of the interferometer phase shift. The eye diagrams at each photodiode are shown in Fig. 10 (left). Their difference, obtained by an oscilloscope math function, i.e., the differentially decoded signal, is seen in Fig. 10 (right). The Q factor is 24 dB for CSRZ pulses. 8-ps-long RZ pulses were also tried and yielded a $Q > 28$ dB.

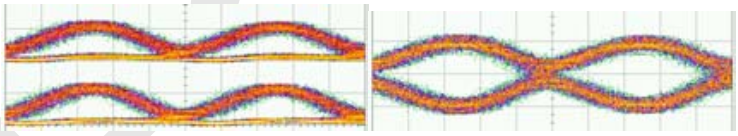

Fig. 10. Back-to-back eye diagrams at interferometer outputs, and difference signal.

The CSRZ-DPSK signal was also transmitted over 58 km of SSMF, 33 km of DSF, and some DCF. **D** Because of a large negative residual CD at the 1547-nm DFB laser wavelength, an external cavity laser was used and tuned to 1560 nm. The Q factor after transmission was > 22 dB.

D Author: What is DSF, DCF?

The CD monitoring hardware of the DPSK setup is very similar to that for intensity modulation, but the clock-phase error signal itself was processed for convenience. CD was monitored by inserting various fiber pieces. Figure 11 shows the CD readout as a function of true CD in the range $DL = -91$ ps/nm $+ \cdots +$ 147 ps/nm ($\gamma = -0.37, \ldots, 0.6$). Again, the readout is fairly linear in the range where the eye diagram is open. The sign of the CD is faithfully returned even when the eye diagram is closed (inset Fig. 11) as long as the clock-phase detector works, the PLL locks, and there is a high-enough percentage of correct data decisions.

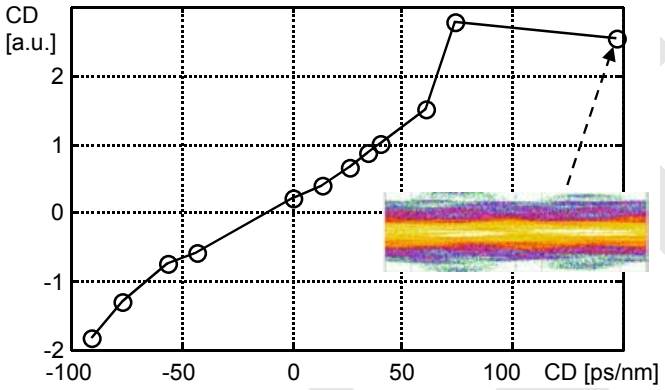

Fig. 11. Chromatic-dispersion detection readout versus actual dispersion. Inset: closed-eye diagram at 147 ps/nm resulting from interferometer output signal difference.

The readout noise at zero CD ranges from 4 ps/nm to < 100 fs/nm for measurement intervals between 38 μs and 157 ms (Fig. 12), with the $2^7 - 1$ PRBS yielding slightly better results than a $2^{23} - 1$ PRBS. In the important range of measurement intervals < 10 ms, the sensitivity is very similar to that of the intensity-modulated system.

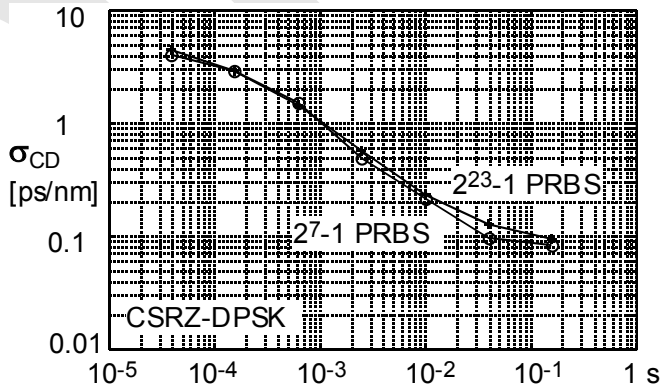

Fig. 12. Standard deviation of measured CD versus measurement interval, at zero actual dispersion.

5. Discussion

Two completely separate data transmission setups were used for the intensity modulation and DPSK experiments. This shows that the CD monitoring scheme does not rely on tricky hardware or luck.

Since the sign of CD is correctly indicated, the error signal could directly control an adaptive CD compensator via an integral controller.

The principle is expected to be scalable to other bit rates: At 10 Gbit/s, one could expect the frequency deviation δf and the modulation frequency to be 4 times smaller, *DL* to be 16 times larger, and the arrival-time modulation $\delta\tau_g$ as well as the measurement interval to be 4 times larger. However, there is no reason why frequency deviation (and modulation frequency) must be lowered. This means that at 10 Gbit/s, a 16 times larger *DL* can probably be measured at least as fast and with at least the same relative accuracy.

Recently, another arrival-time detection scheme of CD has been reported [12], at 10 Gbit/s. However, the arrival-time detection was not synchronous. Our synchronous (lock-in) detection works better for typical measurement intervals that are large against one bit duration. As a consequence, our scheme needs a much smaller frequency modulation. This reduces the parasitic amplitude modulation, is of some importance in densely packed WDM environments, and is a must for DPSK transmission, especially when a long (100 ps) interferometer delay is employed. Moreover, a measurement interval of 10 s was reported in Ref. [12], whereas our scheme responds in submillisecond intervals. This makes it applicable for dynamically routed signals.

6. Conclusions

This chromatic-dispersion (CD) detection scheme is extremely cheap to implement, features superior sensitivity, is fast enough, introduces hardly any transmission penalty, tolerates NRZ, CSRZ, intensity modulation, and DPSK, provides also the sign of CD, and has a very wide measurement range.

References and Links

[1] K. Yonenaga, A. Sano, M. Yonenama, S. Kuwahara, Y. Miyamoto, and H. Toba, "Automatic dispersion equalisation using bit error rate monitoring in 40-Gbit/s optical transmission system," Electron. Lett. **27**, 187–189 (2001).

[2] A. Sano, T. Kataoka, M. Tomizawa, K. Hagimoto, K. Sato, K. Wakita, and K. Kato, "Automatic dispersion equalization by monitoring extracted-clock power level in a 40-Gbit/s, 200-km transmission line," in *Proceedings of the 22nd European Conference on Optical Communication* (IEEE, New York, 1996), pp. 2.207–2.210.

[3] A. B. Sahin, L. S. Yan, Q. Yu, M. Hauer, Z. Pan, and A. E. Willner, "Dynamic dispersion slope monitoring of many WDM channels using dispersion-induced RF clock regeneration," in *Proceedings of the 27th European Conference on Optical Communication* (IEEE, New York, 2001), pp. 446–447.

[4] M. N. Petersen, Z. Pan, S. Lee, S. A. Havstad, and A. E. Willner, "Dispersion monitoring and compensation using a single in-band subcarrier tone," in *Optical Fiber Communication Conference*, Vol. 70 of OSA Trends in Optics and Photonics Series (Optical Society of America, Washington, D.C., 2002), paper WH4.

[5] A. Hirano, S. Kuwahara, and Y. Miyamoto, "A novel dispersion compensation scheme based on phase comparison between two SSB signals generated from a spectrally filtered CS-RZ signal," in *Optical Fiber Communication Conference*, Vol. 70 of OSA Trends in Optics and Photonics Series (Optical Society of America, Washington, D.C., 2002), paper WE2.

[6] Q. Yu, L. S. Yan, Z. Pan, and A. E. Willner, "Chromatic dispersion monitor for WDM systems using vestigial-sideband optical filtering," in *Optical Fiber Communication Conference*, Vol. 70 of OSA Trends in Optics and Photonics Series (Optical Society of America, Washington, D.C., 2002), paper WE3.

[7] V. Mirvoda, D. Sandel, F. Wüst, S. Hinz, and R. Noé, "Linear detection of optical polarization mode dispersion by arrival time modulation," Electr. Eng. **84**,E 71–73 (2002).

←

E Month of magazine?

[8] D. Sandel, V. Mirvoda, F. Wüst, R. Noé, and S. Hinz, "Signed online chromatic dispersion detection at 40 Gb/s with a sub-ps/nm dynamic accuracy," in *Proceedings of the 28th European Conference on Optical Communication* (IEEE, New York, 2002), Vol. 3, p. 6.1.4.

[9] B. Milivojevic, D. Sandel, S. Bhandare, R. Noé, andF. Wüst, "Practical 40-Gbit/s CSRZ-DPSK transmission system with signed online chromatic dispersion detection," in *Proceedings of the 29th European Conference on Optical Communication* (IEEE, New York, 2003), paper Tu3.6.4.

[10] A. F. Elrefaie, R. Wagner, D. Atlas, and D. Daut, "Chromatic dispersion limitation in coherent optical fibre transmission systems," Electron. Lett. **23**, 756–758 (1987).

[11] A. H. Gnauck, G. Raybon, S. Chandrasekhar, J. Leuthold, C. Doerr, L. Stulz, A. Agarwal, S. Banerjee, D. Grosz, S. Hunsche, A. Kung, A. Marhelyuk, D. Maywar, M. Movassaghi, X. Liu, C. Xu, X. Wei, and D. M. Gill, "2.5 Tb/s (64×42.7 Gb/s) transmission over 40×100 km NZDSF using RZ-DPSK format and all-Raman-amplified spans," in *Optical Fiber Communication Conference*, Vol. 70 of OSA Trends in Optics and Photonics Series (Optical Society of America, Washington, D.C., 2002), paper PD FC2.

[12] Y. Takushima, H. Yoshimi, K. Kikuchi, H. Yamauchi, and H. Taga, "Experimental demonstration of in-service dispersion monitoring in 960-km WDM transmission system using optical frequency-modulation method," IEEE Photon. Technol. Lett. **15**, 870–872 (2003).